Colloid Polym Sci (2005) 283: 1007–1015
DOI 10.1007/s00396-004-1259-0

ORIGINAL CONTRIBUTIONS

Tsuneo Okubo
Tomio Yamada
Keisuke Kimura
Akira Tsuchida

Drying dissipative structures of the deionized aqueous suspensions of colloidal silica spheres ranging from 29 nm to 1 μm in diameter

Received: 24 August 2004
Accepted: 2 November 2004
Published online: 19 January 2005

T. Yamada · K. Kimura · A. Tsuchida
Department of Applied Chemistry,
Gifu University, Gifu 501-1193, Japan

T. Okubo (✉)
Institute for Colloidal Organization,
Hatoyama 3-1-112, Uji,
Kyoto 611-0012, Japan
E-mail: okubotsu@ybb.ne.jp
Fax: +81-774-328270

Abstract Macroscopic and microscopic dissipative structural patterns formed in the course of drying a series of the colloidal silica spheres ranging from 29 nm to 1 μm in diameter have been observed in the aqueous deionized suspension on a cover glass. The broad ring patterns of the hill accumulated with the silica spheres are formed around the outside edges in the macroscopic scale for all spheres examined. The spoke-like cracks are also observed in the macroscopic scale and their number decreases sharply as sphere size increases. The pattern area and the time for the dryness have been discussed as a function of sphere size and concentration. The convection flow of water accompanied with that of the silica spheres and interactions among the silica spheres and substrate are important for the macroscopic pattern formation. The microscopic fractal structures of the wave-like patterns and branched strings are formed. Their fractal dimensions are determined. Microscopic patterns form in the narrow range of sphere sizes and concentrations and are determined mainly by the electrostatic and polar interactions between the spheres and/or between the sphere and substrate in the course of solidification.

Keywords Drying dissipative structure · Pattern formation · Colloidal silica spheres · Broad ring · Microscopic fractal pattern

Introduction

Most structural patterns in nature and experiments in the laboratory form via self-organization accompanied with the dissipation of free energy and in the non-equilibrium state. Among several factors in the free energy dissipation, evaporation at the liquid surface and convection induced by the earth's gravity are very important.

In previous papers from our laboratory [1, 2], drying dissipative patterns on a cover glass have been observed for colloidal crystal suspensions of colloidal silica and monodispersed polystyrene spheres. Quite similar macroscopic and microscopic dissipative structural patterns formed between the colloidal silica and polystyrene spheres. The broad ring patterns of the hill accumulated with spheres and the spoke-like and ring-like cracks formed in the macroscopic scale. From these observations existence of the small circle convection cells proposed by Terada [3–5] was supported. The primitive patterns of valleys were formed already in the concentrated suspensions before dryness and they grow toward fine cracks in the course of solidification. Branch-like fractal patterns of the sphere association were observed in the microscopic scale. Capillary forces between spheres at the air–liquid interface and the different rates of convection flows of water and spheres at the drying front were important for the pattern formation. Macroscopic and microscopic structural patterns were studied in the course of drying the suspension of Chinese

black ink on a cover glass and in a dish [6]. The clear broad ring and spoke-like patterns of the rims accumulated with particles formed especially in the central region of the film. For Chinese ink direct observation of the convection flow was successful mainly in a dish.

The drying dissipative structures have been studied further for the linear-type macrocations, i.e., poly(allylamine hydrochloride) [7]. Macroscopic broad ring patterns, where the macroions accumulate densely in the outside edges, formed. Furthermore, beautiful string-like fractal patterns were observed in the microscopic scale. The drying experiments were made for *n*-dodecyltrimethylammonium chloride, which is one of the typical cationic detergent molecules [8]. Broad ring patterns of the hill accumulated with detergent molecules formed around the outside edges of the film in the macroscopic scale. Star-like, blanch-like, arc-like and small block-like microstructures were also observed. Quite recently, drying structural patterns were studied for a series of anionic detergent molecules, sodium *n*-alkyl sulfates (*n*-alkyl = *n*-hexyl, *n*-octyl, *n*-decyl, *n*-dodecyl, *n*-hexadecyl and *n*-octadecyl) [9].

From these studies on drying dissipative structures, macroscopic broad ring patterns for various solutions and suspensions were, surprisingly, similar to each other irrespective of kind of solutes and their concentrations. Microscopic patterns such as branch-like, string-like, arc-like and small block-like ones were, however, reflected in the shape, size and flexibility of the solute molecules. In this work, drying dissipative structure of a series of colloidal silica spheres ranging from 29 nm to 1 μm in diameter in aqueous deionized suspension on a cover glass have been studied systematically as possible. The main purpose of this work is, of course, to study the size effect of the colloidal spheres on the drying dissipative patterns.

Experimental

Materials

Colloidal silica spheres CS22p, CS45, CS82, CS161, CS301 and CS1001 were gift from Catalyst & Chemicals Co. (Tokyo). The diameter (d_o), standard deviation (δ) from the mean diameter and the polydispersity index (δ/d_o) were compiled in Table 1. The values of δ and d_o were determined by the electron microscopy. The surface charge densites of strongly acidic charges of these spheres were determined by the conductometric titration with a Horiba Model DS-14 conductivity meter (Kyoto). These colloidal samples were first purified several times using an ultrafiltration cell (Model 202, Diaflo-XM300 membrane, Amicon Co.), and then deionized with a mixed bed of cation- and anion-exchange resins more than 10 years. It takes a long time before complete deionization is achieved, since the deionization proceeds between the two solid-liquid phases one after another, i.e., between colloidal spheres and water and then water and the resins. It should be noted further that the silica particles are very porous in their surfaces, which is not favorable for the complete deionization process. Water used for the sample preparation was purified by a Milli-Q reagent grade system (Milli-RO5 plus and Milli-Q plus, Millipore, Bedford, MA, USA).

Table 1 Characteristics of colloidal silica spheres used

Sphere	d_o (nm)	δ (nm)	δ/d_o	Charge density (μC/cm^2)
CS22p	29	6	0.21	0.48
CS45	56.3	7.6	0.13	0.30
CS82	103	13.2	0.13	0.38
CS161	183	18.6	0.10	0.47
CS301	311	22.4	0.072	0.40
CS1001	1090	45	0.041	–

Observation of the dissipative structures

An amount of 0.1 mL of the aqueous suspension of the colloidal silica spheres was dropped carefully and gently on a micro cover glass (30 mm×30 mm, thickness No.1, 0.12–0.17 mm, Matsunami Glass Co., Kishiwada, Osaka) in a dish (60 mm in diameter, 15 mm in depth, Petri Co., Tokyo). The cover glass was used without further rinsing in this work. The extrapolated value of the contact angle for pure water was $31 \pm 0.2°$ from the drop profile of a small amount of water (0.2, 0.4, 0.6 and 0.8 μL) on the cover glass. A pipet (1 mL, disposable serological pipet, Corning Lab. Sci. Co.) was used for the dropping. Macroscopic and microscopic observation was made for the film formed after the suspension was dried up completely on a cover glass in a room air-conditioned at 25 °C and 65% in humidity of the air. Concentrations of the silica spheres ranged from 1.33×10^{-7} M to 0.1 M.

Macroscopic dissipative structures were observed with a digital HD microscope (type VH-7000, Keyence Co., Osaka) and a Canon EOS 10 camera with macro-lens (EF 50 mm, $f=2.5$) and a life-size converter EF. Microscopic structures were observed with a laser 3D profile microscope (type VK-8500, Keyence) and a Metallurgical microscope (Axiovert 25CA, Carl-Zeiss, Jena GmbH). Observation of the microscopic patterns was also made with an atomic force microscope (type SPA400, Seiko Instruments).

Results and discussion

Figure 1 shows the typical patterns formed in the drying a series of suspensions of colloidal silica spheres at the

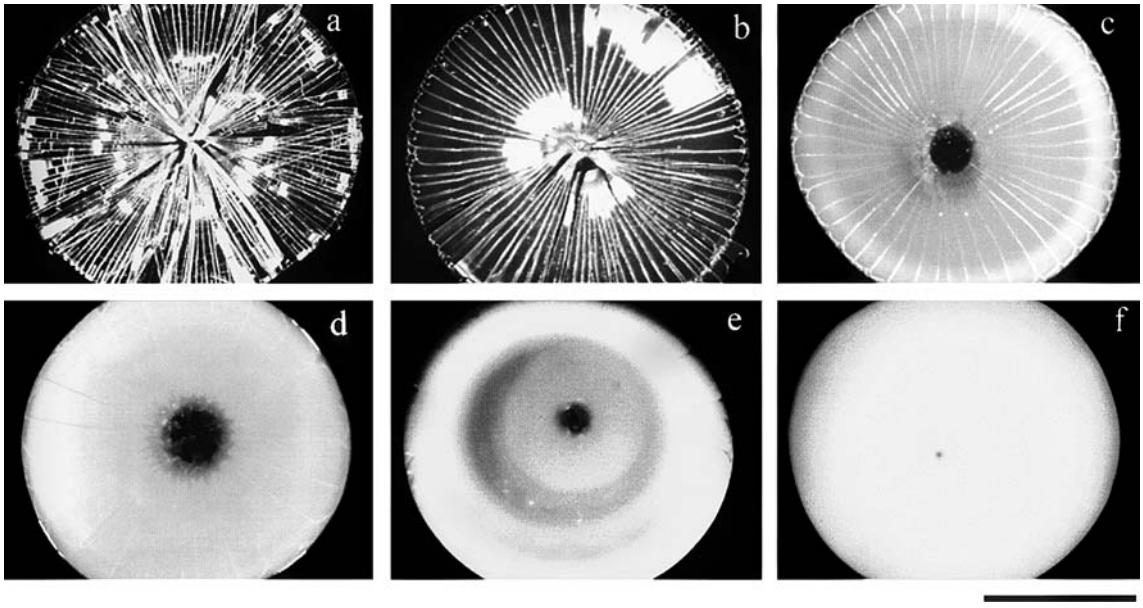

Fig. 1 Patterns formed for colloidal silica spheres at 25 °C. **a** CS22p, **b** CS45, **c** CS82, **d** CS161, **e** CS301, **f** CS1001. In water, $\phi = 0.0333$, 0.1 mL, length of the bar is 5 mm

concentration of 0.0333 in volume fraction (Table 2). The broad rings and the spoke-like cracks were observed. A main cause for the broad ring formation is due to the convection flow of the solvent and the colloidal spheres at different rates under gravity. Especially, flow of the spheres from the center area toward the outside edges in the lower layer of the liquid drop, which was observed on a digital HD microscope directly from the movement of the very rarely occurred aggregates of the spheres, is important [6]. The flow will be enhanced by the evaporation of water at the liquid surface, resulting lowering of the suspension temperature in the upper region. When the spheres reach the edges of the drying frontier at the outside region of the liquid, a part of the spheres will turn to upward and go back to the center region. However, movement of the most spheres may stop at the frontier region by the disappearance of water. This process must be followed by the broad ring-like accumulation of the spheres near the round edges. It

Table 2 Angles between the neighbored cracks (θ) for silica spheres at 25 °C. In water, 0.1 mL

ϕ	θ (degree)				
	CS22p	CS45	CS82	CS161	CS301
0.00133	0.7	1.9	–	–	–
0.0133	1.2	2.7	4.0	8.6	12
0.0333	2.9	4.6	7.4	14	21
00667	4.9	4.2	8.0	40	33
0.1	6.3	7.4	9.0	45	90

should be noted that the broad ring formation was observed for all the solutions and suspensions examined by our group [1, 2, 6–13] and further by other researchers [14–16]. Recently, microgravity experiments were made for the drying dissipative patterns of deionized suspension of colloidal silica spheres [17]. Surprisingly, the broad ring patterns did not disappear even in microgravity. This supports that both the gravitational and the Marangoni convections contribute for the broad ring formation on earth but only the latter is still important in microgravity.

The spoke-like cracks are also observed in the figure clearly in the macroscopic scale and their number decreases sharply as sphere size increases at the same sphere concentration in volume fraction. Increase in sphere size will result in the increase in the elastic modulus of the film and then in the decrease in the crack number.

Figure 2 shows the patterns formed in the drying suspensions of CS45 spheres (56.3 nm in diameter) at the sphere concentrations ranging from 1.33×10^{-7} to 0.1 in volume fraction. The length of the bar is 5 mm. At low sphere concentrations the round islands of sphere regions appeared leaving a small amount of spheres at the outside ridges. At the higher sphere concentrations than 1.33×10^{-3} in volume fraction, the broad rings formed in the outside regions and the spoke-like cracks grew from the outside edge toward the center. Clearly the cracks formed in the process of solidification and shrinking of the wetted films [1, 2]. Number of the cracks decreased as sphere concentration increased. This observation supports that increase in sphere concentration results in the thickening and then hardening of the film. These macroscopic patterns are quite similar to those observed in this work for CS83 spheres, though

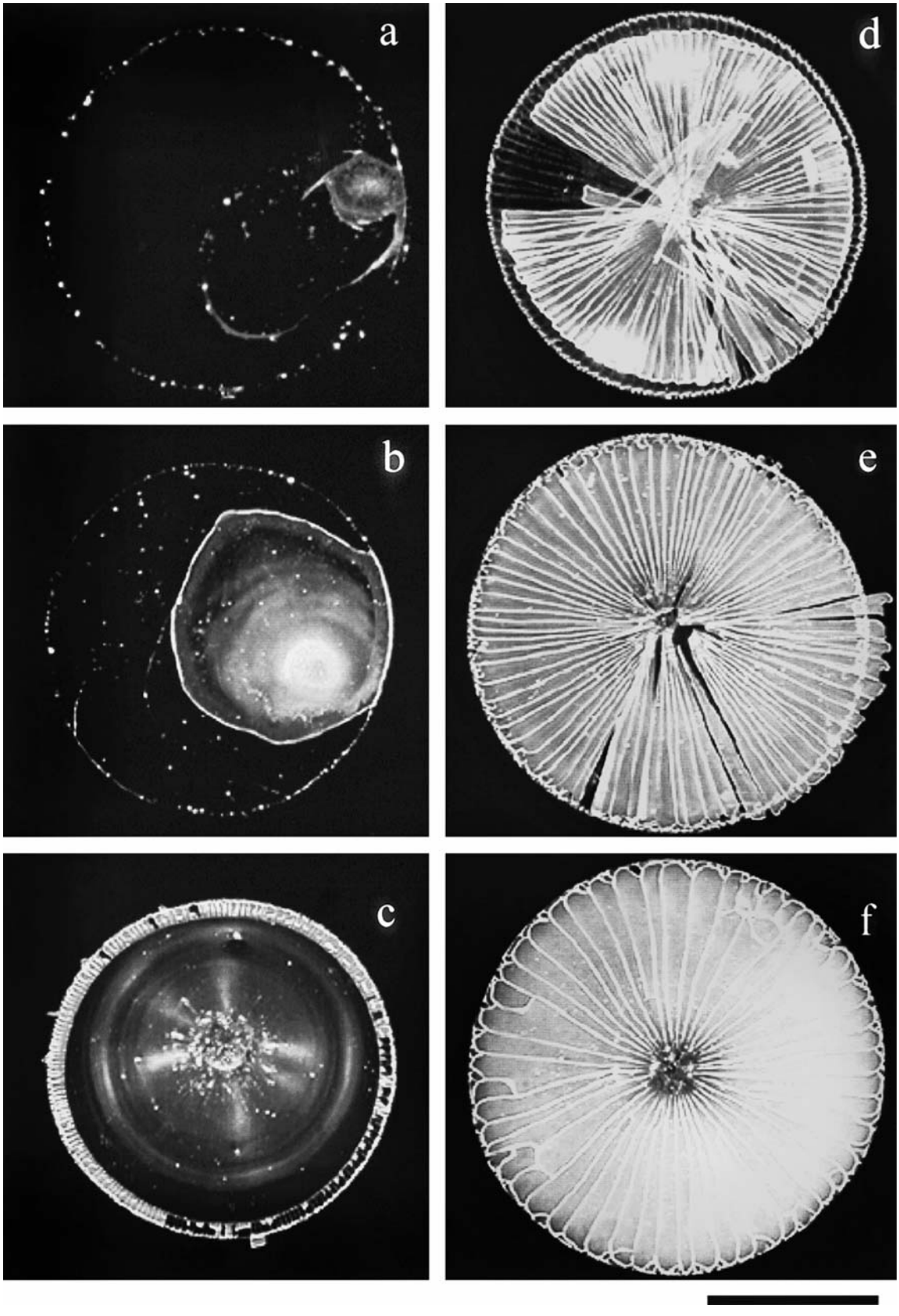
a
d
b
e
c
f

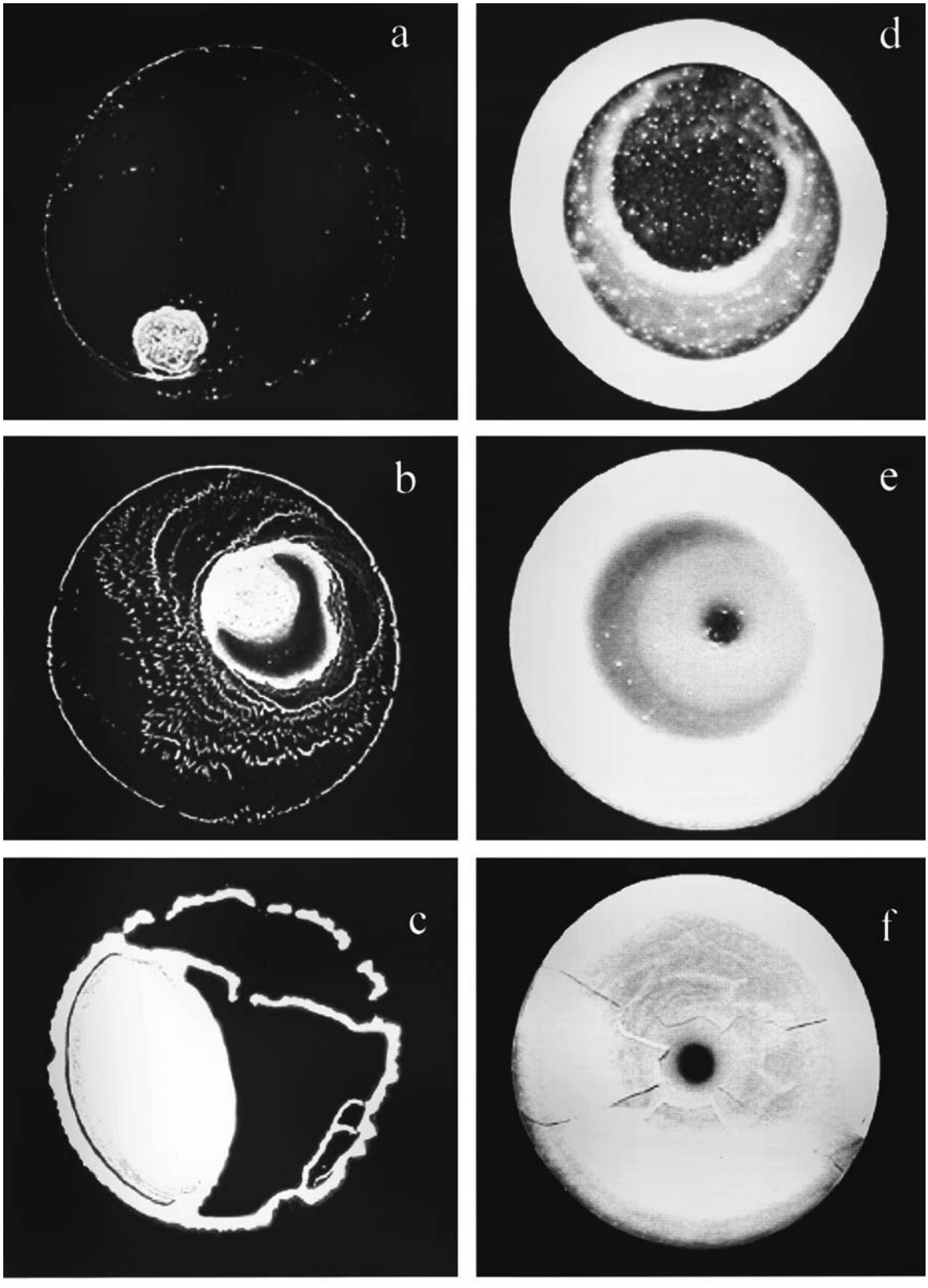

◀

Fig. 2 Patterns formed for CS45 spheres at 25 °C. **a** $\phi = 1.33\times10^{-7}$, **b** 1.33×10^{-5}, **c** 1.33×10^{-3}, **d** 0.0133, **e** 0.0333, **f** 0.1. In water, 0.1 mL, length of the bar is 5 mm

Fig. 3 Patterns formed for CS301 spheres at 25 °C. **a** $\phi = 1.33\times10^{-7}$, **b** 1.33×10^{-5}, **c** 1.33×10^{-3}, **d** 0.0133, **e** 0.0333, **f** 0.1. In water, 0.1 mL, length of the bar is 5 mm

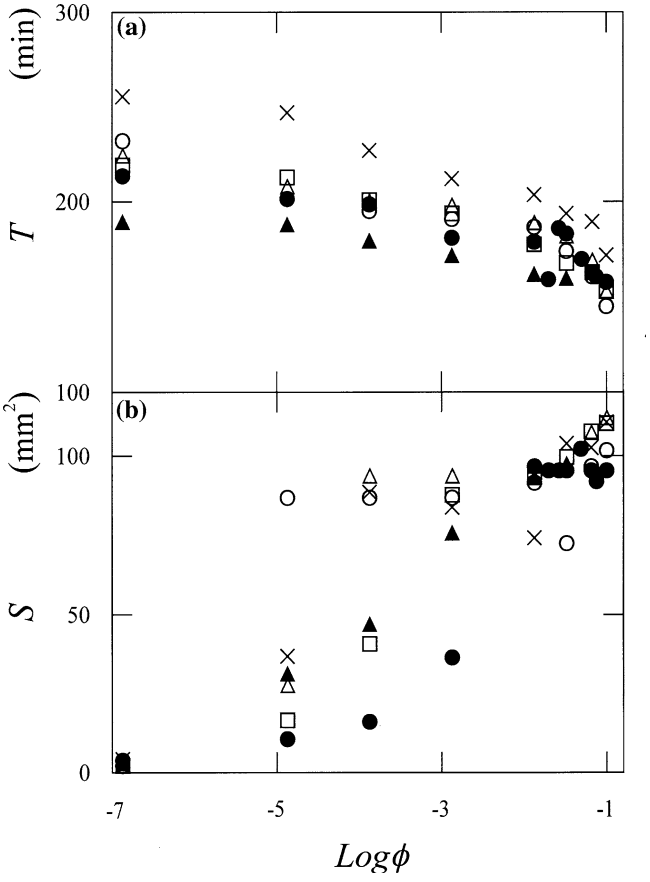

Fig. 4 Drying time (T) and area (S) for colloidal silica spheres as a function of concentration (ϕ) at 25 °C. In water, 0.1 mL, *O* CS22p, *X* CS45, *triangle* CS82, *square* CS161, *filled circle* CS301, *filled triangle* CS1001

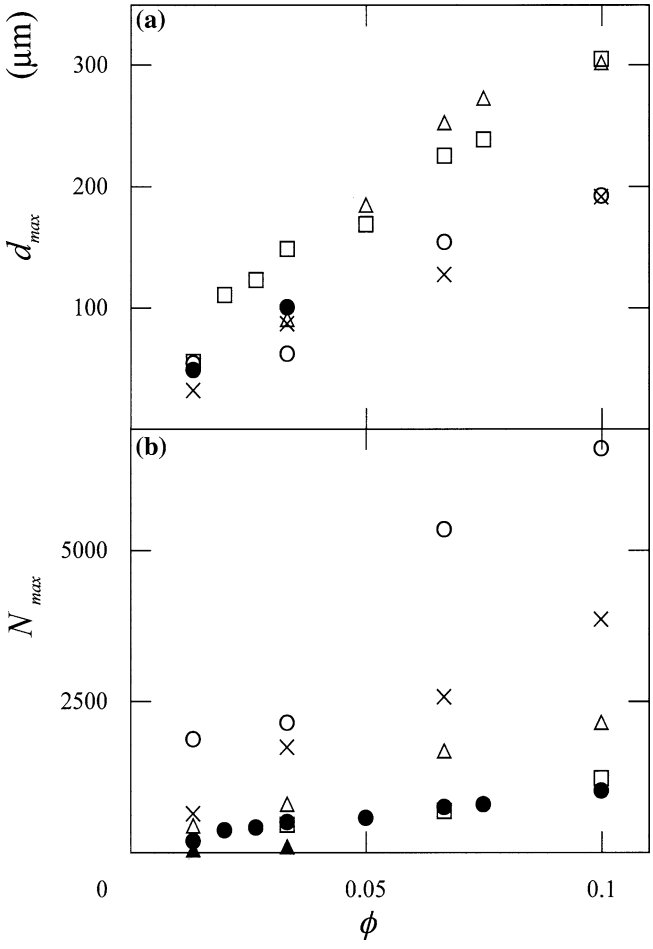

Fig. 6 Thickness maximum (d_{max}) and maximum number of particle layers (N_{max}) for colloidal silica spheres as a function of concentration (ϕ) at 25 °C. In water, 0.1 mL, *O* CS22p, *X* CS45, *triangle* CS82, *square* CS161, *filled circle* CS301, *filled triangle* CS1001

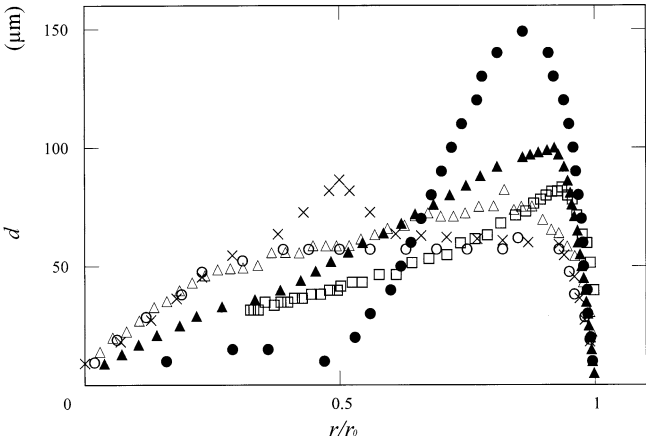

Fig. 5 Thickness (d) for colloidal silica spheres as a function of r/r_o at 25 °C. In water, 0.1 mL, $\phi = 0.0333$, *O* CS22p, $r_o = 4.8$ mm; *X* CS45, 5.75 mm; *triangle* CS82, 4.8 mm; *square* CS161, 5.6 mm; *filled circle* CS301, 6.5 mm; *filled triangle* CS1001, 5.8 mm

showing the pictures were skipped, and also in the previous observation for the same sphere samples [1].

Figure 3 shows the macroscopic patterns for the deionized suspensions of CS301 spheres (311 nm in diameter) at the sphere concentrations ranging from 1.33×10^{-7} to 0.1 in volume fraction. The spoke-like cracks were a quite few. Width of the broad ring at the outside edge increased as sphere concentration increased. It should be noted here that these macroscopic patterns including the other structures such as island formation in the center area were quite similar to each other irrespective of sphere size.

►

Fig. 7 Patterns formed for colloidal silica spheres at 25 °C. In water, **a, e** CS45, $\phi = 1.33\times10^{-5}$; **b , f** CS82, 1.33×10^{-5}; **c, g** CS301, 1.33×10^{-4}; **d, h** CS1001, 1.33×10^{-5}. In water, 0.1 mL, length of the bar: **a–d** 5.0 mm, **e–g** 50 μm, **h** 15 μm

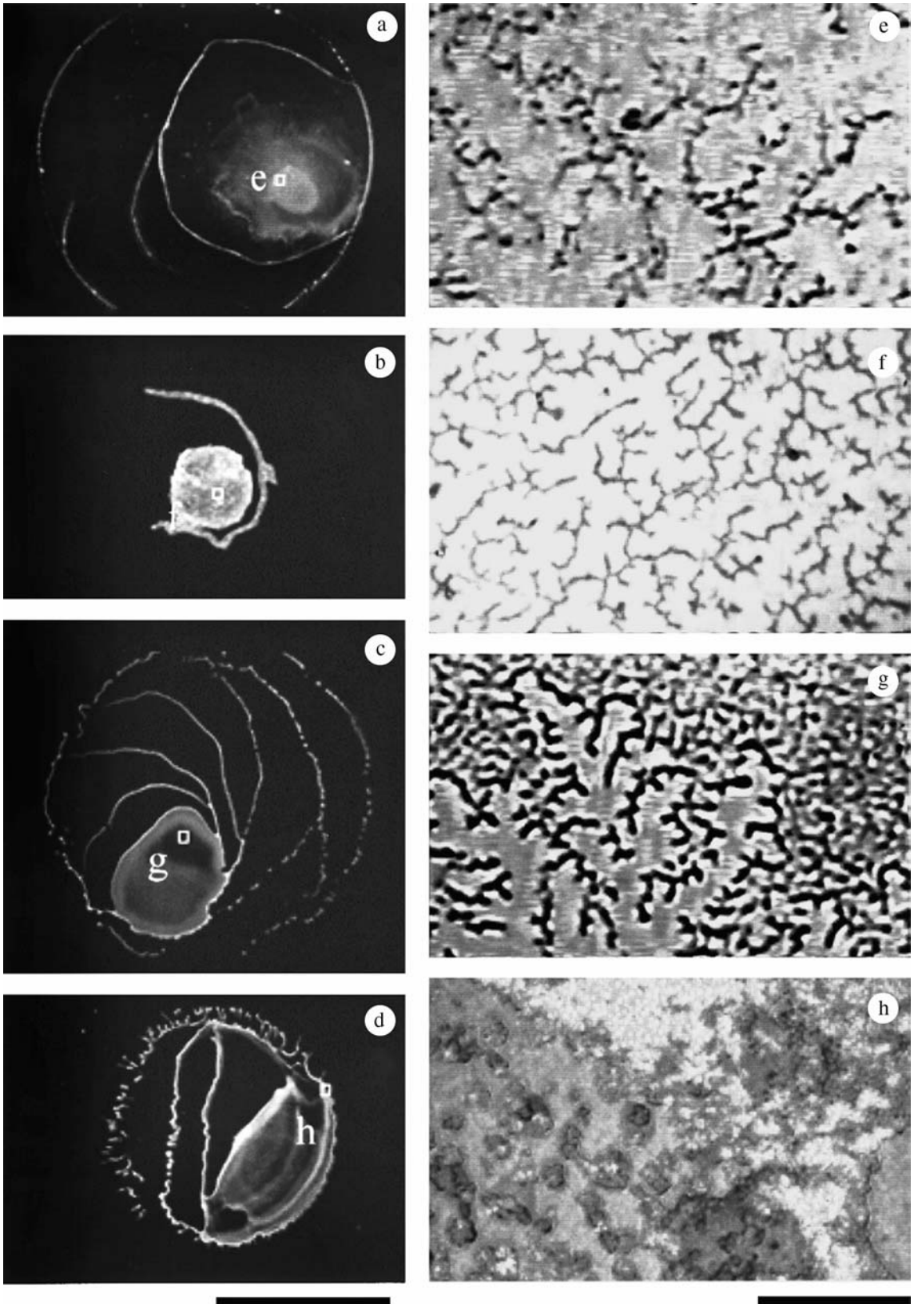
a
e
b
c
g
d
h
e
f
g
h

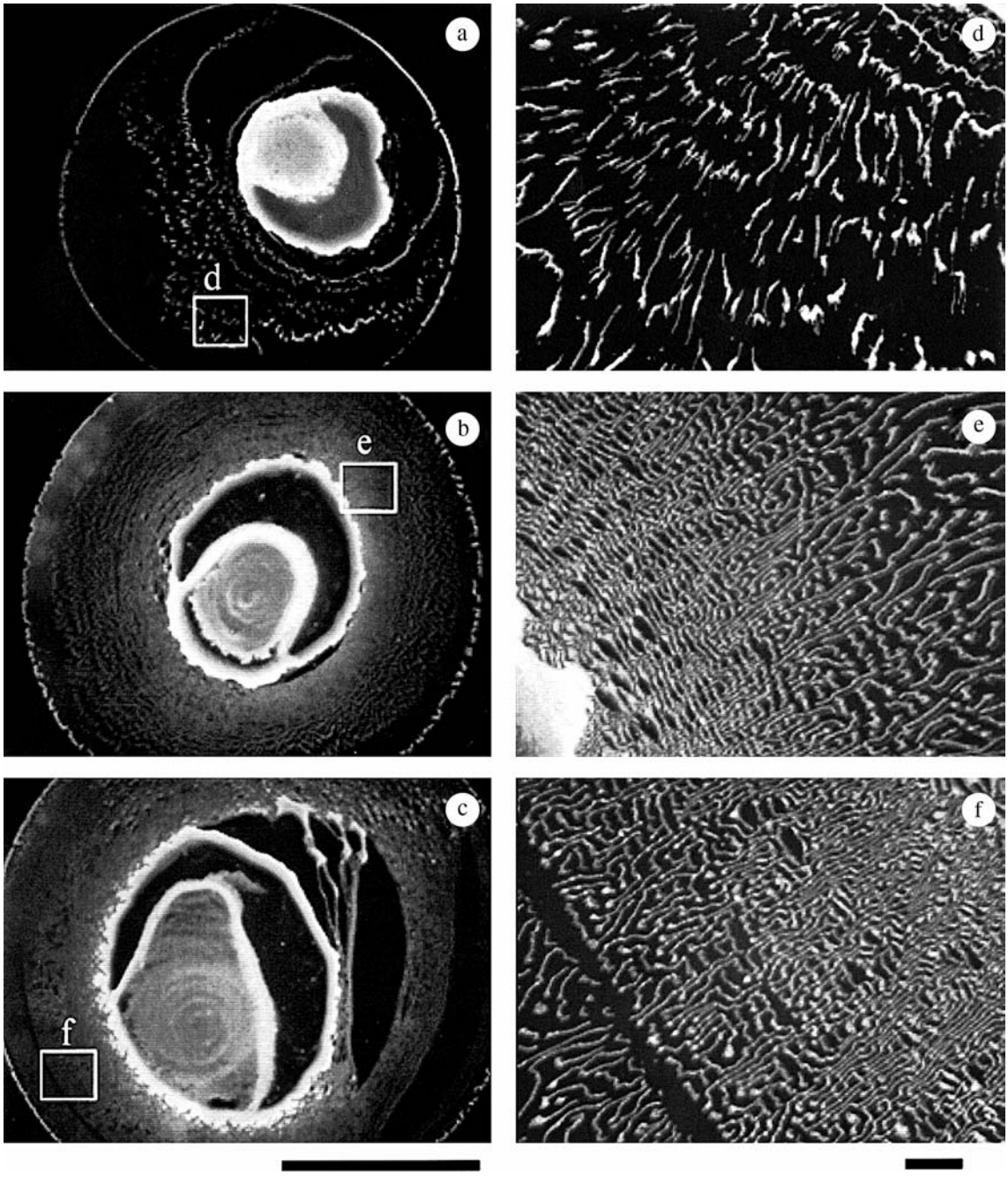

Fig. 8 Patterns formed in the drying process of CS301 at 25 °C. In water, $\phi = 1.33\times10^{-5}$, **a, d** 0.1 mL, **b, e** 0.15 mL, **c, f** 0.2 mL, length of the bar: **a–c** 5.0 mm, **d–f** 200 μm

Figure 4 shows the time for their completion of the dryness observed with the naked eyes, T and the final area of the dried patterns, S as a function of sphere concentration. T decreased as sphere concentration increased, whereas S increased with increasing sphere concentration. These tendencies will be explained with decrease in the surface tension of the suspension as sphere concentration increases [18]. It is clear that T decreases sharply when S increases, which is well understood because the drying process comes fast when the liquid film is thin even the area is large. Furthermore, T-values decreased as the sphere size increased, though the experimental errors were rather large.

Figure 5 shows the thickness of the film as a function of the ratio of the distance from the center (r) against the radius of the circular dried film (r_o). The experiments were made directly using a laser 3D profile microscope. Clearly, the d versus r/r_o profiles became sharp as sphere

Table 3 Fractal dimensions of the micro-structures observed for silica spheres

Sphere	ϕ					
	1.33×10^{-7}	1.33×10^{-5}	1.33×10^{-4}	1.33×10^{-3}	3.33×10^{-3}	0.133
CS22p	–	–	–	–	–	–
CS45	–	1.3	–	–	–	–
CS82	–	1.2	1.3	1.3	1.1	–
CS161	–	–	–	–	–	–
CS301	–	–	1.2	–	–	–
CS1001	–	–	–	–	–	–

size increased, and then turn to broad passing a sharpest profile for CS301 spheres. The convection flow of the spheres toward outside the edges from the center, which is opposite direction of water flow, will be effective for large spheres. For small spheres, on the other hand, flow of spheres will be accompanied with the water flow easily. For the largest spheres examined in this work, 1 μm in diameter, however, the convection flow of the spheres must be slow compared with the flow rate of water convection in the suspension drop on a cover glass.

Figure 6 shows the maxima in the film thickness, d_{max} and the number of sphere layers, N_{max} as a function of sphere concentration, ϕ. The d_{max}- and N_{max}-values increased sharply as the sphere concentration increased. It should be noted here that d_{max} increased as sphere size increased whereas N_{max} decreased with increasing sphere size at the same sphere concentration. These dependencies of d_{max} and N_{max} are quite understandable, because the number of spheres increase sharply as sphere size decreases and sphere concentration increases.

Let's discuss the microstructures observed for the suspensions of silica spheres of various sizes. Figure 7 compares the typical examples of the macro-structures (a, b, c and d) and the corresponding micro-structures (e, f, g and h) for silica spheres ranging from 56 nm to 1090 nm in diameter. Branch-like fractal patterns were observed except CS1001 spheres. Figure 8 shows the microstructures observed for CS301 spheres at the liquid amount of 0.1, 0.15 and 0.2 mL. Patterns were quite similar to each other. It should be noted that the fractal patterns were formed only the limited conditions of sphere sizes and concentrations as is clearly shown in Table 3. Generally speaking, these fractal patterns appeared often on the area, where there are not a lot of spheres enough to cover. The fractal dimensions of the patterns were 1.2 ± 0.1 and insensitive to sphere size and sphere concentration.

Acknowledgements Dr. M. Komatsu and Dr. H. Nishida of Catalysts & Chemicals Ind. Co. (Tokyo) are thanked deeply for their providing a series of monodispersed colloidal silica samples ranging from 29 nm to 1090 nm in diameter.

References

1. Okubo T, Okuda S, Kimura H (2002) Colloid Polym Sci 280:454
2. Okubo T, Kimura K, Kimura H (2002) Colloid Polym Sci 280:1001
3. Terada T, Yamamoto R, Watanabe T (1934) Sci Paper Inst Phys Chem Res Jpn 27:173; Proc Imper Acad Tokyo 10:10
4. Terada T, Yamamoto R, Watanabe T (1934) Sci Paper Inst Phys Chem Res Jpn 27:75
5. Terada T, Yamamoto R (1935) Proc Imper Acad Tokyo 11:214
6. Okubo T, Kimura H, Kimura T, Hayakawa F, Shibata T, Kimura K (2004) Colloid Polymer Sci 283:1–9
7. Okubo T, Kanayama S, Ogawa H, Hibino M, Kimura K (2004) Colloid Polym Sci 282:230
8. Okubo T, Kanayama S, Kimura K (2004) Colloid Polym Sci 282:486
9. Kimura K, Kanayama S, Tsuchida A, Okubo T Colloid Polymer Sci (submitted)
10. Okubo T, Onoshima D, Kimura K, Tsuchida A (in preparation)
11. Okubo T, Hibino M, Ogawa H, Kimura K, Tsuchida A (in preparation)
12. Okubo T, Togawa H, Kimura K, Tsuchida A (in preparation)
13. Okubo T, Yamaguchi T, Otake A (in preparation)
14. Ohara PC, Heath JR, Gelbart WM (1997) Angew Chem 109:1120
15. Ohara PC, Heath JR, Gelbart WM (1998) Langmuir 14:3418
16. Gelbart WM, Sear RP, Heath JR, Chang S (1999) Faraday Discuss 112:299
17. Tsuchida A, Nakagawa N, Yoshikura K, Okamoto J, Itoh M, Okubo T, publication in preparation
18. Okubo T (1988) J Colloid Interf Sci 125:386